

# Effects of multilevel phase masks on interpixel cross talk in digital holographic storage

M.-P. Bernal, G. W. Burr, H. Coufal, R. K. Grygier, J. A. Hoffnagle, C. M. Jefferson, E. Oesterschulze, R. M. Shelby, G. T. Sincerbox, and M. Quintanilla

We study the interpixel cross talk introduced to digital holographic data storage by use of a multilevel phase mask at the data-input plane. We evaluate numerically the intensity distribution at the output detector for Fourier plane hologram storage in a limited-aperture storage medium. Only the effect at an output pixel of interpixel cross talk from the four horizontal and vertical neighboring pixels is considered, permitting systematic evaluation of all possibilities. For random two-level and pseudorandom six-level phase masks, the influence of the pixel fill factor, as well as the aperture size of the storage medium, is studied. Our simulations show that, for a given aperture size, a random two-level mask is more susceptible to interpixel cross talk than is a pseudorandom six-level mask. Decreasing the pixel fill factor below 94% with a pseudorandom six-level phase mask makes it theoretically possible to have a system with no errors from interpixel cross talk if one particular 5-pixel pattern is forbidden through modulation coding. Reducing the input fill factor below 85% means that no patterns need to be excluded.

© 1997 Optical Society of America

*Key words:* Holographic storage, interpixel cross talk, phase masks.

## 1. Introduction

Digital holographic data storage was proposed shortly after the discovery of holography.<sup>1</sup> In recent years, a widespread effort has been made to reduce the concept to practice.<sup>2-8</sup> The idea consists of storing a large number of arrays of picture elements or pixels. Each pixel is either ON or OFF to encode a binary 1 or 0. Every array or page is stored in an optically sensitive medium as a grating that results from the interference between the object beam and a reference beam. For storing a large number of pages in the same volume and retrieving them independently, various multiplexing techniques can be used.<sup>7</sup> All the pixels in a data page can be read in parallel, which results in a potential data rate of the order of

gigabits per second. Moreover, the theoretical limit on the volume density is  $V/\lambda^3$ , where  $V$  is the volume of the material and  $\lambda$  the wavelength of the light illuminating the medium.

One of the most desirable configurations in holographic data storage is the Fourier transform configuration, as shown in Fig. 1. This configuration has many advantages over other geometries deriving from the translational invariance of the Fourier transform and because the stored information is dispersed over a large volume of the recording medium. This has several system implications, such as removability of the media, insensitivity to local defects, immunity to dust, etc. Information is input into the holographic storage system with a programmable pixel device called a spatial light modulator (SLM). This device is placed in the front Fourier plane of lens  $L_1$  and illuminated with an expanded and collimated laser beam, called the object beam. The holographic storage medium, which in this case has a cross-sectional area  $D^2$ , is located in the common Fourier plane of lenses  $L_1$  and  $L_2$ , where the two-dimensional spatial Fourier transform of the SLM data pattern is formed. When the focal lengths of both lenses are equal, a system with unity magnification (a  $4f$  system) is obtained.

A hologram is stored when an interference pattern produced in the medium by superposition of the ob-

---

M.-P. Bernal, G. W. Burr, H. Coufal, R. K. Grygier, J. A. Hoffnagle, C. M. Jefferson, R. M. Shelby, and G. T. Sincerbox are with the Almaden Research Center, IBM Research Division, 650 Harry Road, San Jose, California 95120-6099. E. Oesterschulze is with the Institute of Technical Physics, University of Kassel, Heinrich-Plettstrasse 40, 34132 Kassel, Germany. M. Quintanilla is with the Departamento de Fisica Aplicada, Facultad de Ciencias, Universidad de Zaragoza, 50009 Zaragoza, Spain.

Received 30 September 1996; revised manuscript received 13 January 1997.

0003-6935/97/143107-09\$10.00/0

© 1997 Optical Society of America

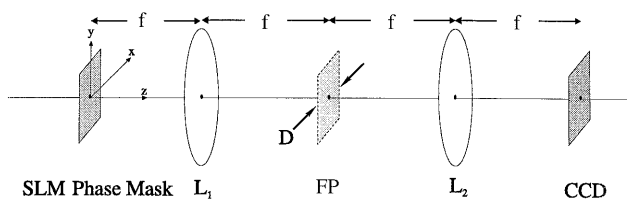


Fig. 1. Digital holographic data-storage system in a  $4f$  configuration. In this study, the SLM and the phase mask are considered perfectly aligned and in the object Fourier plane of the lens  $L_1$ . The storage medium, with a cross section  $D^2$ , is located in the common Fourier plane (FP) of the lenses  $L_1$  and  $L_2$ . The CCD camera is placed in the image Fourier plane of  $L_2$ . A hologram is formed when the object beam and the reference beam interfere in the holographic storage medium.

ject beam with the reference beam creates an identical modulation index of refraction as a result of the photosensitivity of the storage medium. To recover the digital information, the object beam is reconstructed by illumination of the storage medium with the same reference beam that was used for recording. Lens  $L_2$  performs an inverse Fourier transformation of the reconstructed object beam, causing the desired two-dimensional data pattern to be imaged at the output of the  $4f$  system. A CCD camera with the proper pixel spacing can then receive an entire data page in parallel.

Holography in a Fourier transform configuration has a very important drawback: Intensity variations of orders of magnitude can occur in the Fourier plane. In digital holographic storage systems, the information displayed on the SLM is encoded as an array of ON and OFF pixels. The periodicity of the pattern (independent of the input data) creates large intensity peaks in the Fourier transform plane. These intensity peaks, which convey little information, tend to saturate the material, while the information-rich low-intensity regions are recorded only weakly. A uniform distribution of object beam intensities in the Fourier plane would permit optimal use of both the beam ratio between reference and signal (which improves diffraction efficiency) and the limited intensity range for linear response (necessary for fidelity between reconstruction and input).

A more homogeneous energy distribution can be obtained in the Fourier plane by use of phase masks.<sup>9–12</sup> A common variant is a matrix of phase apertures with the same pixel spacing as the SLM. Each aperture in this matrix is of constant phase, randomly selected from the set  $\Phi_n = 2\pi n/N$ , with  $n = 0, \dots, N - 1$ . If this random  $N$ -level phase mask is placed in proximity to and aligned with the SLM, diffraction effects from the phase mask are minimized. Since the CCD array is not phase sensitive, the phase mask does not modify the information encoded by the SLM when the object beam is imaged onto the CCD during hologram reconstruction. The high-intensity peak is now spread more uniformly over the Fourier transform plane owing to the random phase distribution of the SLM phase pixels.

Thus, the phase mask allows the dynamic range of the medium to be used more effectively without losing the benefits of storage in the Fourier plane.

Burckhardt<sup>9</sup> was the first to introduce the concept of a two-level phase mask to overcome the problem of nonuniform intensity distributions. Phase masks produced with two phase steps have the advantage of being simpler to manufacture than multilevel phase steps, but they do not reduce the variance of the irradiance distribution in either the hologram plane or the reconstructed image plane as effectively.<sup>11</sup> Therefore, there is much interest in studying phase masks with a higher number of levels.

For practical applications, it is important to minimize the bit error rate of the retrieved digital data. Because of distortions coming from lens aberrations and diffraction from apertures, as well as distortion introduced by the holographic storage process, light originating from one SLM pixel can be spread to CCD pixels adjacent to the intended target. As a result of this, the integrated intensity on the corresponding CCD pixel can have an intermediate value between 1 and 0. For some particular SLM pattern combinations, the data cannot be decoded correctly because of the ambiguous CCD output signals. This is called interpixel cross talk.<sup>13</sup> For the purposes of this paper, we assume that the optical system has diffraction-limited lenses of infinite extent and that the only distortions are due to diffraction effects from the cross-sectional aperture of the storage medium. Therefore, at the CCD plane the image of each SLM pixel consists of a main lobe and a series of sidelobes extending across the entire CCD plane. This is shown in Fig. 2, where the output signal of one SLM pixel is plotted versus CCD pixel locations for three different storage-medium apertures (described by the ratio  $f/D$ ). The coherent superposition of these lobes from several neighboring pixels can give rise to interpixel cross talk. Note that large  $f/D$  values correspond to small apertures, and consequently significant diffraction at the output planes.

Recently, Hong *et al.*<sup>14</sup> studied the effect of random two-level phase masks on interpixel cross talk by examining all possible 5-pixel combinations. For that study, a SLM with a 100% fill factor was assumed (that is, the width of the active area of the pixel equals the pixel spacing). They showed that some amplitude–phase combinations can cause interpixel cross talk. Identifying those patterns and avoiding them with appropriate modulation coding realizes a system with zero errors from interpixel cross talk at the same storage density.

In this paper, we present a flexible numerical method for evaluating interpixel cross talk. Using our simulation, we can model any number of phase levels in the phase mask and examine SLM fill factors less than 100%. For this particular study, the effects of random two-level and pseudorandom six-level phase masks on interpixel cross talk are analyzed as a function of the linear fill factor of the SLM, as well as various spatial cutoff frequencies in the Fourier transform plane. In Fig. 3, we show a cross

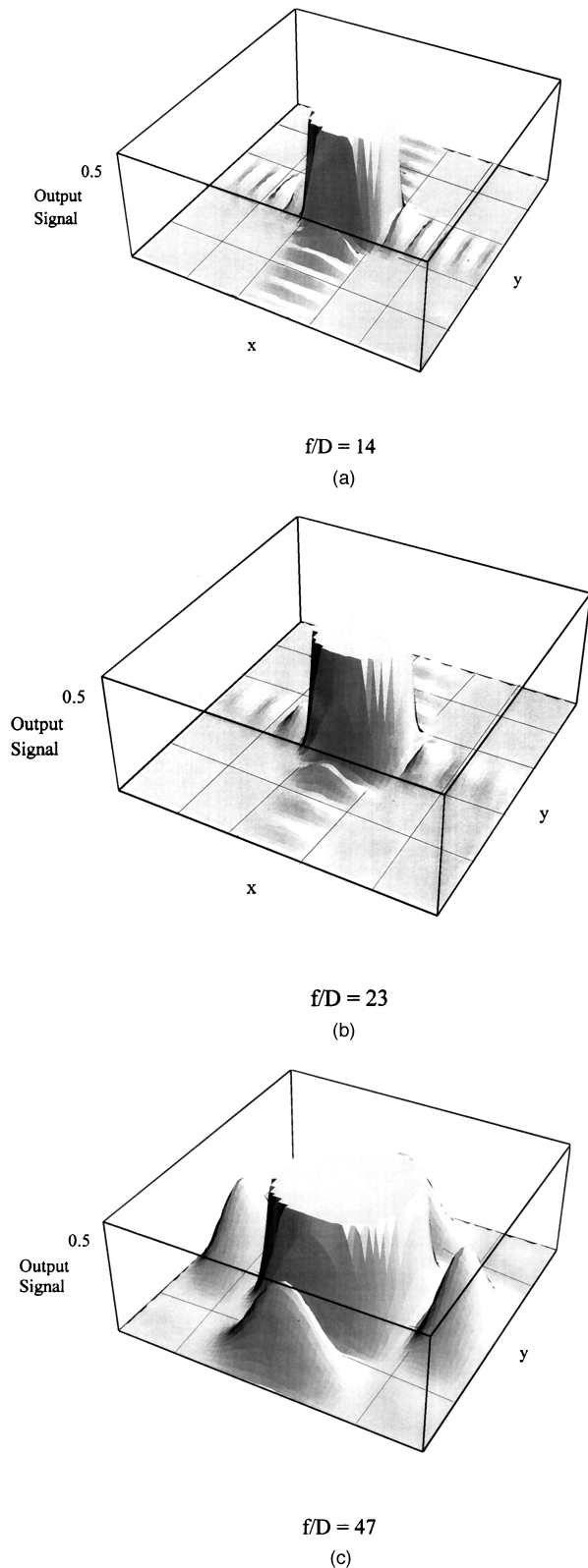


Fig. 2. Output signal of a single SLM pixel in the CCD plane for three different aperture sizes: (a)  $f/D = 14$ , (b)  $f/D = 23$ , and (c)  $f/D = 47$ . The signal consists of a main lobe and a series of smaller sidelobes extending in the  $x$  and  $y$  axes of the plane. The signals have been normalized to 1 and only a range from 0 to 0.5 is shown to emphasize the lower-signal lobes. The structure is due to the diffraction effect from the cross-sectional area of the storage medium, which is acting as a low-pass spatial filter.

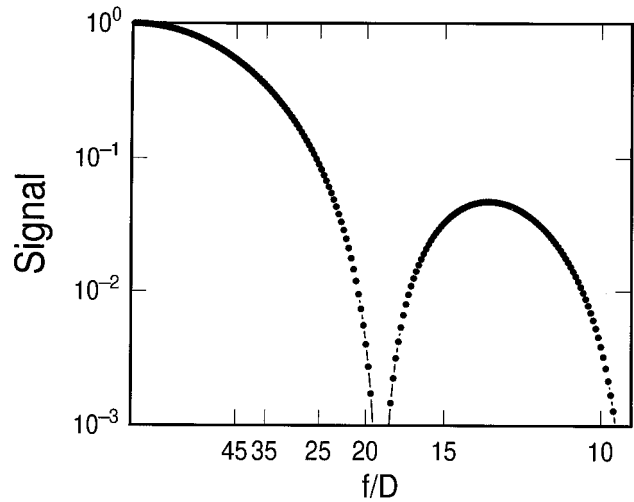


Fig. 3. Intensity of the Fourier spectrum of one SLM pixel as a function of the ratio  $f/D$ .

section of the Fourier spectrum of one SLM pixel plotted as a function of the ratio  $f/D$ .

With a pseudorandom six-level phase mask, the phase shift between pixel closest neighbors is constrained to be  $\pm\pi/3$ . This mask is of more interest than a completely random six-level mask for several reasons:

1. Allowing phase shifts of only  $\pm\pi/3$  avoids large diffraction effects caused by  $\pi$ -phase steps.
2. Worst-case amplitude-phase combinations obtained with a truly random six-level phase mask are covered by the case of a two-level phase mask, which we discuss in detail below.
3. Pseudorandom six-level phase masks perform better in the reconstructed image than do masks with fewer levels.<sup>12</sup>

It is important to note that our comparison between systems with and without phase masks does not include the expected loss of fidelity resulting from the nonlinear effects of the storage medium when storing holograms in the Fourier transform plane without a phase mask.

## 2. Review of the Method

To study interpixel cross-talk noise caused by pixels from the same SLM phase-mask page, we consider the system model described in Fig. 1. The SLM and the phase mask are assumed to be an array of  $(2P_1 + 1)$  by  $(2P_2 + 1)$  square apertures with a periodicity  $\Gamma$  in each direction. In this study, we consider the phase pixels to be in physical contact and aligned with respect to the SLM pixels, so that light from any phase pixel illuminates only one SLM pixel. One could do this, for example, by imaging the SLM onto the phase mask or vice versa.

For uniform plane-wave illumination and a 100% fill factor, the transmission-field amplitude of the SLM phase mask directly after the phase mask is

given by

$$U_0(x, y, z = 0) = \sum_{m=-P_1}^{P_1} \sum_{n=-P_2}^{P_2} c_{mn} \exp(i\Phi_{mn}) \times \text{rect}\left(\frac{x - m\Gamma}{\Gamma}\right) \text{rect}\left(\frac{y - n\Gamma}{\Gamma}\right), \quad (1)$$

where  $c_{mn}$  can take values of 0 or 1 and  $\Phi_{mn}$  varies between 0 and  $2\pi$ . Using Rayleigh–Sommerfeld diffraction theory<sup>15</sup> yields the electric-field amplitude in the Fourier transform plane of lens  $L_1$ :

$$U_c(x, y, z = 2f) = \frac{i\Gamma^2}{\lambda f} \sum_{m=-P_1}^{P_1} \sum_{n=-P_2}^{P_2} c_{mn} \exp(i\Phi_{mn}) \times \exp\left[-\left(\frac{i2\pi xm\Gamma}{\lambda f}\right)\right] \exp\left[-\left(\frac{i2\pi yn\Gamma}{\lambda f}\right)\right] \times \text{sinc}\left(\frac{\Gamma x}{\lambda f}\right) \text{sinc}\left(\frac{\Gamma y}{\lambda f}\right), \quad (2)$$

where  $\lambda$  is the laser wavelength,  $f$  is the focal length of lenses  $L_1$  and  $L_2$ , and

$$\text{sinc}(x) \equiv \begin{cases} 1 & x = 0 \\ \sin(\pi x)/\pi x & \text{otherwise.} \end{cases} \quad (3)$$

If diffraction-limited lenses of infinite extent are assumed, the aperture stop of the system is given by the range of Fourier components passing through the focal plane of lens  $L_1$ . For Fourier plane holographic data storage, this range is determined by the cross-sectional area of the storage medium. We control the range of frequency components by imposing a square aperture:

$$P(x, y) = \text{rect}(x/D) \text{rect}(y/D), \quad (4)$$

where  $D$  is the width of the aperture. Assuming perfect registration on the CCD array and again making use of scalar diffraction theory yields the electric field  $U_d(x, y, z = 4f)$ :

$$U_d(x, y, z = 4f) = -\Gamma^2 \sum_{m=-P_1}^{P_1} \sum_{n=-P_2}^{P_2} c_{mn} \exp(i\Phi_{mn}) \times I(x + m\Gamma) I(y + n\Gamma), \quad (5)$$

where

$$I(r) = \int_{-\alpha}^{+\alpha} \text{sinc}(\Gamma s) \exp(-i2\pi r s) ds, \quad (6)$$

and  $\alpha \equiv D/2\lambda f$ .

As expected, each square input SLM phase pixel is transformed at the output into a convolution of the square with a two-dimensional sinc function as a result of diffraction from the aperture of the storage medium (sometimes called the point-spread function). The summation represents the coherent superposition of the central lobe of the desired pixel with the appropriate sidelobes of all neighboring pixels. In the unity magnification system assumed in

this paper, the pixel spacing of the CCD array is the same as that of the SLM phase mask. We need to integrate the intensity value  $|U_d(x, y, z = 4f)|^2$  over the corresponding center detector pixel to obtain the output signal of the pixel.

To evaluate the real and imaginary parts of the electrical field at the Fourier plane of lens  $L_1$  and at the CCD plane, we use the fast Fourier transform algorithm.<sup>16</sup> We divide every SLM phase pixel into  $(2M + 1)^2$  subpixels to create an input matrix with  $(2P_1 + 1)(2P_2 + 1)(2M + 1)^2$  elements. The output matrix has the same number of elements. We show below that the accuracy of the algorithm depends on the number of subdivisions per pixel, as well as the number of pixels in the matrix. Subdividing the pixel into small square apertures also allows us to vary the fill factor of the SLM pixels. This permits the study of practical SLM's in which the active area of the pixel does not fill the area assigned to each SLM pixel. For example, the Meadowlark Optics Model RSLM-360K SLM has a linear fill factor of 87.5%. The Displaytech Model ICO256C SLM is manufactured with a linear fill factor of 93%.

Because of the discrete nature of the fast Fourier transform, the range of storage-medium apertures that can be modeled is determined by the number of pixels in the input matrix. For analyzing any arbitrary aperture size, the input-matrix dimension has to be large, resulting in excessive computational time. Consequently, there is a trade-off between the speed of computation and the freedom of choice in apertures that can be used to study interpixel cross-talk effects.

### 3. Numerical Results

Because of diffraction from the storage-medium aperture, the energy of every data-phase pixel spreads over the CCD plane as a main lobe and a series of decreasing intensity sidelobes that extend along the  $x$  and  $y$  axes, as shown in Fig. 2. In principle, all the pixels in the SLM phase plane are required for evaluating the output signal in the CCD plane of a particular data-phase pixel. However, the main contribution comes from the nearest-neighbor pixels.

To show the influence of distant SLM pixels on the evaluation of each output signal at the CCD plane, we computed the output signal of a single SLM pixel located at  $x = y = z = 0$ . The fraction of output power that is spread to the neighboring pixels of the target output CCD pixel ( $x = y = 0, z = 4f$ ) was evaluated for different values of the ratio  $f/D$ . The various pixel locations are shown in Fig. 4. Note that only one triangle has to be computed since the point-spread function is symmetric. In Fig. 5, the fractional power is plotted versus CCD pixel location for several values of  $f/D$ . The contrast between undesired and desired signals falls to 1% for diagonal neighbors [location (1, 1)] even for small storage-medium cross-sectional apertures. The contrast between the target and its horizontal–vertical neighbors [pixel (1, 0)] is approximately 10%. From this we conclude that the horizontal–vertical neigh-



Fig. 4. CCD pixel locations in which signal power is computed for a single input SLM pixel, to show roll-off of the point-spread function.

neighbors are of primary interest for determining inter-pixel cross talk. We should note, however, that considerations based on the data of Fig. 5 do not include the effects of coherent summation. Our approach is to use the 5-pixel structures to identify

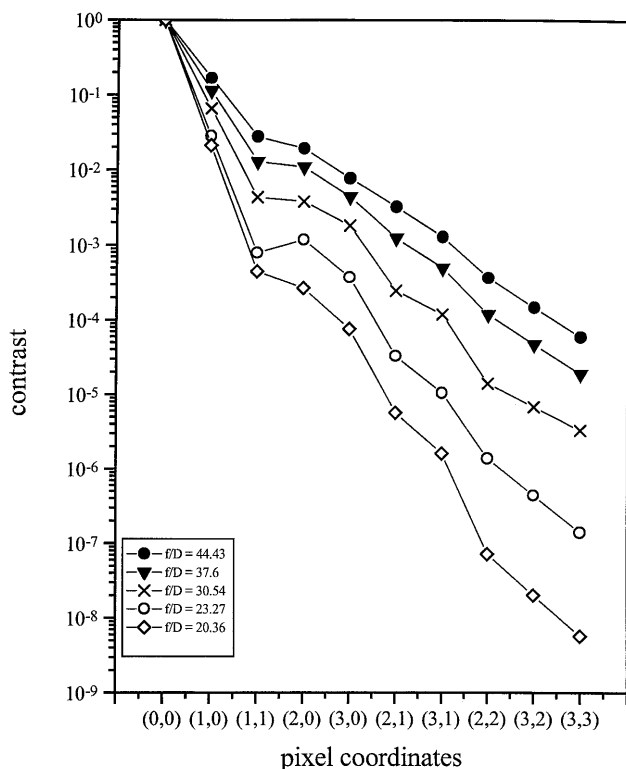


Fig. 5. Neighbor-to-center contrast evaluated in the CCD pixel locations shown in Fig. 4 for several storage-medium cross-sectional apertures.

outright exclusion patterns, in which interpixel cross talk is unavoidable, as well as to estimate the effects of the fill factor on the remaining patterns. The next logical step would be to add diagonal and other neighbors to the worst-case 5-pixel patterns, which we leave for a later paper.

For the numerical evaluations, the wavelength  $\lambda$  was taken to be 532 nm, the focal length of both lenses  $f = 80$  mm, and  $\Gamma = 20 \mu\text{m}$ . Note, by looking at Eq. (6), that the results depend only on  $\Gamma$  and the ratio  $D/2\lambda f$  and are independent of the particular values of  $D$ ,  $\lambda$ , and  $f$ . Also note that, as  $f/D$  gets larger, the cross-sectional area becomes smaller or, equivalently, the volumetric storage-density increases.

If a random two-level phase mask is used, there are 13 different data-phase configurations of the four neighboring pixels for each of the three possible states of the central pixel  $(0, 1^+, 1^-)$ . Figure 6 shows these 13 patterns for the case of a 0 central pixel. For the 1 pixels, a superscript plus indicates 0 phase and a superscript minus means  $\pi$  phase. When we refer to these patterns, the letter indicates the amplitude-phase configuration of the four closest neighbors of the central pixel, while the superscript indicates the amplitude and phase of the central pixel in the pattern.

In the case of a pseudorandom six-level phase mask (the phase step between adjacent pixels can be only  $\pm\pi/3$ ) the 13 different amplitude-phase configurations are the same as those for a two-level phase mask. However, there are now only two possible states for the central pixel  $(0, 1)$ . Thus, neighboring 1 pixels with a plus sign in Fig. 6 have a phase shift of  $+\pi/3$  with respect to the central pixel, while a minus represents a phase shift of  $-\pi/3$ . According to our representation, in this case the superscript can be only 0 or 1.

The accuracy of our numerical algorithm is influenced by both the number of subdivisions per data-phase pixel and the number of 0 pixels enclosing the patterns. The effect of the number of subdivisions is shown in Fig. 7 for pattern  $I^{1+}$ . The signal value asymptotically converges to 1.00429, so the margin of error at 13 subdivisions per pixel is approximately 0.07%. In the following computations from Eq. (6),  $13 \times 13$  subdivisions per SLM phase pixel were used when the output signal versus  $f/D$  was evaluated. Subdivisions of  $51 \times 51$  were used in the calculations involving fill factors. If we increase the number of pixels surrounding each pattern and the output signal is similarly evaluated, the discrepancy at  $30 \times 30$  pixels is 0.03% of the asymptotic value.

The number of 0 pixels that are added around each pattern also determines the set of apertures that can be simulated (because it sets the resolution of the matrix in the Fourier transform plane where the aperture is imposed). For instance, if the 5-pixel patterns are placed in a  $30 \times 30$  input grid, the possible values of  $f/D$  (within the range of values applicable for holographic storage devices) are immediately con-

Pattern Label	A <sup>0</sup>	B <sup>0</sup>	C <sup>0</sup>	D <sup>0</sup>	E <sup>0</sup>	F <sup>0</sup>	G <sup>0</sup>	H <sup>0</sup>	I <sup>0</sup>	J <sup>0</sup>	K <sup>0</sup>	L <sup>0</sup>	M <sup>0</sup>
SLM/phase pattern													

Fig. 6. Thirteen unique patterns of neighbor pixels considered in this study for the evaluation of interpixel cross talk, shown for the case of a central 0. For the case of a two-level phase mask, there are 26 more similar patterns corresponding to a central pixel 1 and phase 0 (superscript plus) or a central pixel 1 and phase  $\pi$  (superscript minus). In the case of a six-level phase mask there are only 13 additional patterns, corresponding to a central pixel 1 and no phase. For the pseudorandom mask, a plus or a minus in neighboring pixels represents a phase shift of  $\pm\pi/3$  with respect to the central pixel.

strained to 14.6, 20.4, 21.2, 22.2, 23.3, 24.4, 25.7, 27.1, 28.7, 30.5, 32.6, 34.9, 37.6, and 40.7.

#### 4. Two-Level Phase Mask

First, a two-level phase mask with a 100% fill factor is studied. The 39 unique output-signal values have been numerically computed for several storage-medium apertures ( $f/D = 14.6, 20.4, 21.2, 22.2, 23.3, 24.4, 25.7, 27.1, 28.7, 30.5, 32.6, 34.9, 37.6, 40.7$ ). There is no overlap between the output signal 0 patterns and the 1 patterns for values of  $f/D$  smaller than  $\approx 35$ . The first errors at the CCD appear for  $f/D = 34.9$ , when the highest output-signal value for a central 0 pixel is 0.251 (pattern L<sup>0</sup>), and the lowest signal value for a central 1 pixel is 0.157 (pattern I<sup>1-</sup>). There are five interpixel cross-talk patterns: I<sup>1-</sup>, F<sup>1-</sup>, H<sup>0</sup>, K<sup>0</sup>, and L<sup>0</sup>. In Fig. 8, the output signals of these five interpixel cross-talk patterns are shown as a function of  $f/D$ . These values are in qualitative agreement with the results obtained by Hong *et al.*<sup>14</sup> At  $f/D = 35$ , they found the same five troublesome patterns plus pattern B<sup>1-</sup>. In our simulations at  $f/D = 34.9$ , we find that, although pattern B<sup>1-</sup> does not actually fall below L<sup>0</sup>, it is quite close (0.27 versus 0.24).

The results for a 100% fill factor, displayed in Fig. 8, show that a system with no intrinsic errors arising

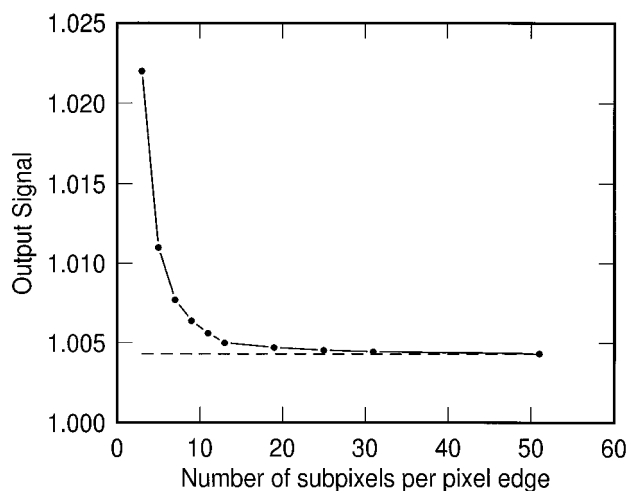


Fig. 7. Output signal of the central pixel in pattern I<sup>1+</sup> by use of a two-level phase mask and  $f/D = 37.6$  plotted versus the number of subdivisions per pixel edge.

from interpixel cross talk can be obtained for  $f/D = 34.9$  if the design of the SLM two-level phase-mask combination excludes patterns I<sup>1-</sup>, F<sup>1-</sup>, H<sup>0</sup>, K<sup>0</sup>, and L<sup>0</sup> from the 39 possible patterns. The next step is to study the interpixel cross-talk performance as the SLM fill factor is varied. Setting the cross-sectional aperture to  $f/D = 37.6$ , there are 10 interpixel cross-talk patterns: I<sup>1-</sup>, F<sup>1-</sup>, B<sup>1-</sup>, C<sup>0</sup>, D<sup>0</sup>, F<sup>0</sup>, H<sup>0</sup>, I<sup>0</sup>, K<sup>0</sup>, and L<sup>0</sup>. These interpixel cross-talk patterns are evaluated for linear fill factors from 20% to 100%.

To give consistency to our results, we normalized, at each fill factor, the output signals of the interpixel cross-talk patterns by the signal of pattern M<sup>1-</sup> (which has the highest output signal). The results are shown in Fig. 9, in which the relative intensity in the central pixel is plotted versus the linear fill factor. Interpolating in Fig. 9 from the computed output signals at linear fill factors of 96.078% and 92.156%, we can see that, at a linear fill factor of 94%, there is a separation between the signals of the patterns corresponding to a central 0 and those corresponding to a central 1, with the only exceptions being pattern L<sup>0</sup>, which always remains in the 1 region, and pattern I<sup>1-</sup>, which only reaches the 1 region for a low linear fill factor, 64%. It follows that, by eliminating the occurrence of patterns L<sup>0</sup> and I<sup>1-</sup> with suitable modulation codes and by having pixels with a linear fill

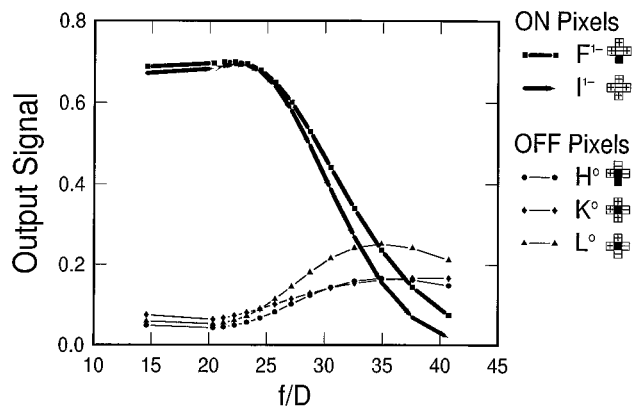


Fig. 8. Output-signal values for the interpixel cross-talk patterns of a two-level phase mask as a function of  $f/D$ . Interpixel cross talk is found for  $f/D$  values greater than or equal to 34.9. In the plot, only the five interpixel cross-talk patterns found for  $f/D = 34.9$  are analyzed, but as  $f/D$  increases above 40 the number of patterns that produce interpixel cross talk increases beyond those shown here.

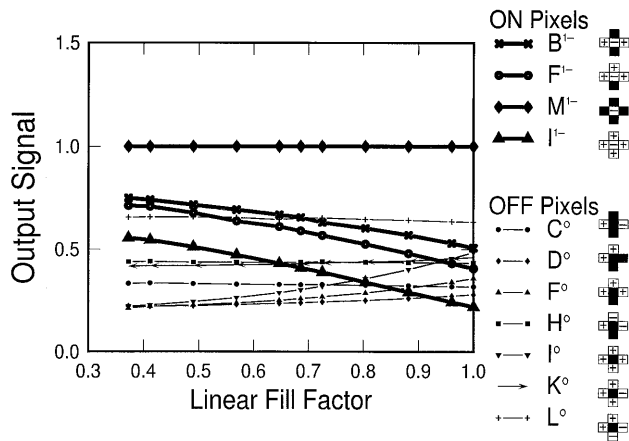


Fig. 9. Output-signal values in the 10 worst-case patterns with a two-level phase mask as a function of the SLM phase pixel fill factor at  $f/D = 37.6$ . If the linear fill factor is less than or equal to 0.94 and patterns  $L^0$  and  $M^{1-}$  are removed, there is no overlap between the 0 and the 1 patterns.

factor equal to or less than 94%, we can achieve a system with no errors arising from interpixel cross talk.

### 5. Pseudorandom Six-Level Phase Mask

Here we analyze pseudorandom six-level phase masks, for which the phase shift between two adjacent pixels is always  $\pm\pi/3$ . For this case, there are 26 different configurations divided into two sets of 13 patterns, corresponding to central pixel 0 or 1. Patterns coincide with those found for a two-level phase mask. It has been shown that these multilevel masks yield a higher signal-to-noise ratio in the reconstructed hologram than do two-level masks.<sup>12</sup>

The 26 output signals were evaluated for different cross-sectional apertures in the storage medium under the physical conditions described in Section 4. When  $f/D = 34.9$ , the maximum output-signal value for the patterns with central pixel 0 is 0.142 (pattern  $K^0$ ), well below the lowest output-signal value (0.429) for the patterns with central pixel 1, (pattern  $M^1$ ).

Interpixel cross-talk errors show up at  $f/D = 43.4$ , when the maximum output-signal value for the patterns with central pixel 0 is 0.286 (pattern  $I^0$ ), whereas the lowest output-signal value obtained for the patterns corresponding to central pixel 1 is 0.262 (pattern  $M^1$ ). This case is shown in Fig. 10, where the signal values for the five worst patterns are plotted as a function of  $f/D$ . A comparison of this plot with that of Fig. 8 shows that, if a pseudorandom six-level phase mask is used instead of a two-level mask, the cross-sectional area at the storage medium can be smaller but still nominally error free. The five interpixel cross-talk patterns shown in Fig. 10 are  $A^1$ ,  $M^1$ ,  $F^0$ ,  $I^0$ , and  $J^0$ .

If the fill factor is changed, the situation becomes analogous to the case of a two-level phase mask. This is shown in Fig. 11, in which the normalized output-signal values corresponding to the five interpixel cross-talk patterns are shown plotted versus the

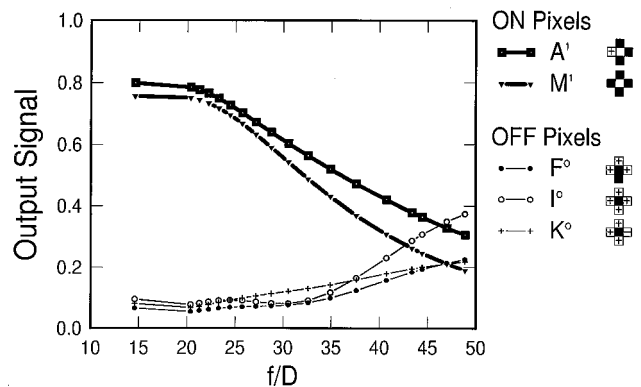


Fig. 10. Output-signal values for the five interpixel cross-talk patterns with a pseudorandom six-level phase mask as a function of  $f/D$ . In contrast to the case of a two-level phase mask, there is no crossover between patterns at  $f/D = 34.9$ . When the value of  $f/D$  is greater than or equal to 43.4, five out of 26 patterns introduce interpixel cross talk.

linear fill factor at  $f/D = 47$ . Again, at an interpolated linear fill factor of 94% there is a separation between the 0 patterns and the 1 patterns after pattern  $M^1$  is excluded. By eliminating it from the data-phase-mask design, we can achieve an error-free holographic system for  $f/D = 47$ . By looking at Fig. 11 one also realizes that pattern  $M^1$  can be kept in the SLM design if pixels with a fill factor less than 85% are used.

### 6. Discussion

To understand the effects of phase masks on interpixel cross talk, we compare the above results with numerical calculations carried out for data patterns with no phase mask. There are only six different patterns (times the two states of the central pixel: 1 or 0), as shown in Fig. 12. The letters have the same meanings as for the previous cases, but now subscripts are used to indicate the amplitude of the

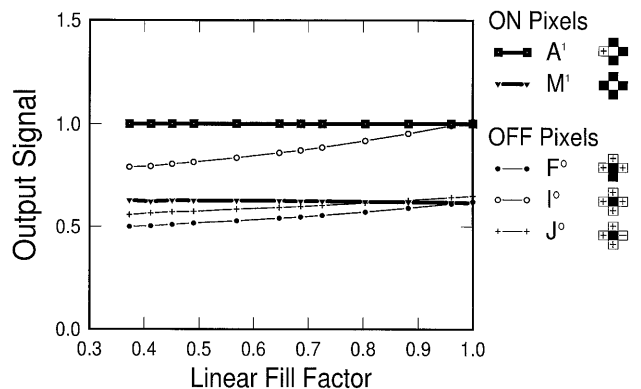


Fig. 11. Output-signal values for the five interpixel cross-talk patterns plotted versus the SLM phase pixel fill factor. In this case,  $f/D = 47$  and a pseudorandom six-level phase mask is used. A system with no intrinsic errors is nominally achieved by elimination of pattern  $M^1$  for a linear fill factor less than 0.94. An error-free system can also be obtained without eliminating any patterns if the SLM pixel fill factor is less than 85%.

Pattern Label	A <sub>0</sub>	B <sub>0</sub>	D <sub>0</sub>	F <sub>0</sub>	I <sub>0</sub>	M <sub>0</sub>
SLM pattern						

Fig. 12. Six unique amplitude-only 5-pixel patterns. Note that there is no phase information in the patterns. As before, there are six additional patterns for a central 1 pixel.

central pixel in the pattern. For these binary intensity patterns at  $f/D = 37.6$ , there is a significant gap between the 0 and the 1 signals. In Fig. 13, the output signals of these 12 patterns are shown for linear fill factors from 20% to 100%. There are no errors from interpixel cross talk in any of the cases. This indicates that the interpixel cross-talk effects we have described are primarily due to the introduction of the phase mask in the holographic system and are not just from the cross-sectional apertures. However, the benefits of phase masks outweigh the disadvantages of not having them, and we have shown here that the interpixel cross-talk performance of the phase masks can be improved by the following:

1. Excluding a few patterns from the design with suitable modulation codes of the SLM pixels.
2. Using lower fill factors (found in practical systems anyway).
3. Using pseudorandom multilevel codes.

The analysis of Hong *et al.*<sup>14</sup> focused on the interpixel cross-talk effects produced by a two-level phase mask with a 100% fill-factor data mask. Our simulations find quantitative agreement within a normalization constant that depends on  $f/D$ . This factor turns out to be the fraction of energy that passes

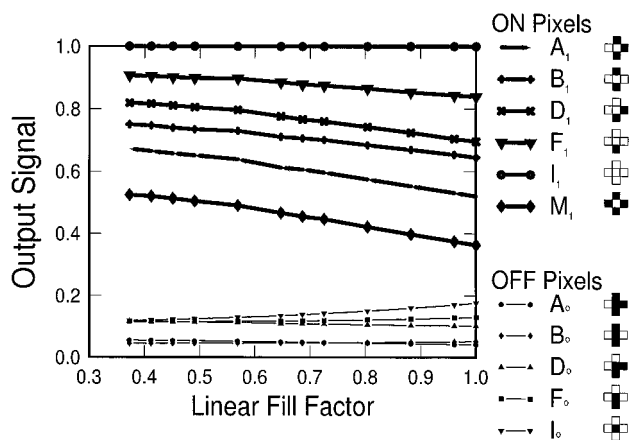


Fig. 13. Output-signal values for the 12 different no-phase-mask patterns plotted as a function of the fill factor for  $f/D = 37.6$ . (In the graph there are only 11 patterns since pattern M<sub>0</sub>, corresponding to the five OFF pixels, is always zero). No errors from interpixel cross talk are seen when there is no phase mask in the system.

through the aperture in the Fourier transform plane. The need for this normalization constant can be seen by application of the conservation of energy principle. For example, for pattern I<sup>1+</sup> Hong *et al.*<sup>14</sup> obtained an output signal of 1.53, with the energy from an input pixel integrated across the image plane taken to be unity. Pattern I<sup>1+</sup> corresponds to all five pixels ON, with the same phase. Visualizing a SLM with all the pixels ON results in the value of the output signal at each CCD pixel being 1.53, leading to an increase in total energy. The output-signal value for the same pattern obtained with our method, under the same physical conditions, is 0.937. We plan to perform experiments in the IBM HOST (holographic optical storage tester<sup>7</sup>) to compare with these simulation results.

## 7. Conclusions

In this paper, we have investigated the influence of two-level and pseudorandom six-level phase masks on the interpixel cross talk of a holographic storage system in the Fourier transform configuration as a function of the storage-medium cross-sectional area and the SLM fill factor. For a SLM two-level phase mask and  $f/D = 37.6$ , a nominally error-free system can be achieved by a decrease in the linear fill factor to less than or equal to 94% and avoidance of two particular patterns with modulation coding. In contrast, a pseudorandom six-level phase mask does not experience errors as a result of interpixel cross talk until the value of  $f/D$  reaches 43.4. For a value of  $f/D = 43.4$  and a linear SLM fill factor less than or equal to 94%, a system with no intrinsic errors can be obtained by elimination of only one of the interpixel cross-talk patterns. If the fill factor is decreased below 85%, an error-free system can be obtained even with all 26 possible 5-pixel combinations. If the input SLM had more than two signal levels, the results obtained in this paper could be used to arrange the input so as to create a true binary pattern at the output detector array.

Using this numerical algorithm, we intend to pursue the study of other effects, such as misregistration of the detector array or the phase pixels and the effects of additional neighboring pixels on the results presented here. Further study is also needed to develop algorithms that will allow us to investigate important problems such as defocused pixels, magnification, tilting, etc.

This research was supported in part by the U.S. Advanced Research Project Agency under agreement MDA972-94-2-008. We want to thank in particular Roger Macfarlane, Harald Günther, Jonathan Ashley, and Brian Marcus from the IBM Research Division, Almaden Research Center, and John Hong, Ian McMichael, and Jian Ma from the Rockwell Science Center for their input.

## References

1. P. J. van Heerden, "Theory of optical information storage in solids," *Appl. Opt.* **2**, 393-400 (1963).

2. L. Hesselink and M. Bashaw, "Optical memories implemented with photorefractive media," *Opt. Quantum Electron.* **25**, 611–651 (1993).
3. F. Mok, "Angle-multiplexed storage of 5000 holograms in lithium niobate," *Opt. Lett.* **18**, 915–917 (1993).
4. J. Heanue, M. Bashaw, and L. Hesselink, "Volume holographic storage and retrieval of digital data," *Science* **265**, 749–752 (1994).
5. G. Sincerbox, "Holographic storage revisited," in *Current Trends in Optics*, C. Dainty, ed. (Academic, New York, 1994), pp. 195–207.
6. G. W. Burr, F. H. Mok, and D. Psaltis, "Angle and space multiplexed holographic storage using 90 degree geometry," *Opt. Commun.* **117**, 49–55 (1995).
7. M.-P. Bernal, H. Coufal, R. K. Grygier, J. A. Hoffnagle, C. M. Jefferson, R. M. Macfarlane, R. M. Shelby, G. T. Sincerbox, P. Wimmer, and G. Wittmann, "A precision tester for studies of holographic optical storage materials and recording physics," *Appl. Opt.* **35**, 2360–2373 (1996).
8. G. W. Burr, F. H. Mok, and D. Psaltis, "Storage of 10,000 holograms in LiNbO<sub>3</sub>:Fe," in *Conference on Lasers and Electro-Optics (CLEO'96)*, Vol. 9 of OSA Technical Digest Series (Optical Society of America, Washington, D.C., 1994), paper CMB7, p. 9.
9. C. B. Burkhardt, "Use of a random phase mask for the recording of Fourier transform holograms of data masks," *Appl. Opt.* **9**, 695–700 (1969).
10. B. Hill, "Some aspects of a large capacity holographic memory," *Appl. Opt.* **11**, 182–191 (1972).
11. W. C. Stewart, A. H. Firester, and E. C. Fox, "Random phase data masks: fabrication tolerances and advantages of four phase level masks," *Appl. Opt.* **11**, 604–608 (1972).
12. Y. Nakayama and M. Kato, "Diffuser with pseudorandom phase sequence," *J. Opt. Soc. Am.* **69**, 1367–1372 (1979).
13. X. Yi, P. Yeh, and C. Gu, "Statistical analysis of cross-talk noise and storage capacity in volume holographic memory," *Opt. Lett.* **19**, 1580–1582 (1994).
14. J. Hong, I. McMichael, and J. Ma, "Influence of phase masks on cross talk in holographic memory," *Opt. Lett.* **21**, 1694–1696 (1996).
15. J. W. Goodman, *Introduction to Fourier Optics* (McGraw-Hill, New York, 1968).
16. E. O. Brigham, *The Fast Fourier Transform* (Prentice-Hall, New York, 1974).